

electron temperature by 300°K with application of the lowest-power heating wave used.) Also listed in Table I are the estimated minimum and maximum values of α . These limits result from the numerical fitting procedure, the effect of electron distributions, and the accuracy of the microwave measuring system. If the recombination coefficient is assumed to be of the form $\alpha = \alpha_0 + k_p p$, where p is the pressure, the relevant parameters are

$$\alpha_0 = (1.0^{+1.2}_{-0.6}) \times 10^{-8} \text{ cm}^3 \text{ sec}^{-1},$$

$$k_p = (6.6^{+9.1}_{-5.5}) \times 10^{-10} \text{ cm}^3 \text{ sec}^{-1} \text{ Torr}^{-1},$$

where the errors quoted were obtained by considering all errors in α as systematic.

In summary, the net rate of decay of free electrons was observed to be very similar to that observed by previous investigators; however, we found that a consistent model of the plasma must include a free-electron generation term. The pressure-dependent term in the net recombination coefficient is evidently too large to be fully accountable to the presence⁶ of He_3^+ or to collisional stabilization as described by Bates⁷ for hydro-

gen. We believe that the pressure dependence may result from atomic collisional stabilization of autoionizing levels via curve crossing in the He_3^* system. The size of the measured α also indicates that dissociative recombination of He_2^+ may have been prematurely discounted.²

*Work supported by the U. S. Atomic Energy Commission.

¹J. B. Gerardo and M. A. Gusinow, Phys. Rev. A **3**, 255 (1971).

²J. R. Bardsley *et al.*, in *Advances in Atomic and Molecular Physics*, edited by D. R. Bates (Academic, New York, 1970), Vol. 6, p. 17.

³C. B. Wharton, in *Plasma Diagnostic Techniques*, edited by R. H. Huddleston and S. L. Leonard (Academic, New York, 1965), p. 500.

⁴M. A. Heald and C. B. Wharton, *Plasma Diagnostics with Microwaves* (Wiley, New York, 1965), Chap. 4.

⁵A. V. Phelps and J. P. Molnar, Phys. Rev. **89**, 1202 (1953).

⁶M. A. Gusinow, R. A. Gerber, and J. B. Gerardo, Phys. Rev. Lett. **25**, 1248 (1970).

⁷D. R. Bates and S. P. Khare, Proc. Phys. Soc., London **85**, 231 (1965).

Correlation Effect and Double Electron Ejection in the Photoabsorption Process*

T. N. Chang, T. Ishihara, and R. T. Poe†

Physics Department, University of California, Riverside, California 92502

(Received 24 February 1971)

Within the framework of many-body perturbation theory, a calculation has been carried out for the process of double electron ejection in photoabsorption, $\gamma + \text{Ne}(1s^2 2s^2 2p^6) \rightarrow \text{Ne}^{++}(1s^2 2s^2 2p^4) + e + e$. Excellent agreement with experiment has been obtained. The importance of electron-electron correlation and the dominant physical processes involved are discussed.

The study of the dynamic effects of electron-electron correlation constitutes one of the major current research topics in atomic and molecular physics. In this regard the process of double electron ejection (DEE) from atoms by photon impact is particularly interesting. In general, the DEE phenomenon may occur via the following two ways. (1) A two-step process: A single electron ejection (SEE) is followed by an Auger transition of the residual ion. (2) Electron-electron correlations: For DEE with both ejected electrons from the same shell, experiments¹⁻³ have shown that even when mechanism (1) is strictly forbidden because of energy considerations, the magnitude of the DEE process remains large. Elec-

tron-electron correlation effects must be responsible for this effect.

While extensive experimental data on multi-electron photoexcitation are available, an effective theoretical treatment has not been given. However, the special case of helium where process (1) cannot occur has been treated, and effects of ground-state correlations on the DEE process have been examined.⁴ Recently, the Brueckner-Goldstone many-body perturbation-theory (MBPT) approach has been extensively applied to atomic problems⁵ and shown to be particularly useful in treating correlation effects. Here we report the essential results of a first-principles theoretical calculation, based on the

MBPT approach, for the DEE in neon by x rays (278 eV),

$$\gamma + \text{Ne}(1s^2 2s^2 2p^6) \rightarrow \text{Ne}^{++}(1s^2 2s^2 2p^4) + e + e.$$

Our result is in excellent agreement with the experiment of Carlson.¹ In particular, some general features of the DEE process can be understood through a physical interpretation of the contributing diagrams.

Outline of the MBPT calculation and results.

—In the MBPT approach,⁶ the unperturbed Hamil-

tonian of the system is

$$H_0 = \sum_i (T_i + V_i),$$

where the single-particle potential V is chosen to be the V_{N-1} -type Hartree-Fock potential⁵ of the atom. The perturbation,

$$H' = H_\gamma + \sum_{i>j} v_{ij} - \sum_i V_i,$$

contains the interaction with the external photon field H_γ plus the electron-electron correlation terms.

The time-development operator for the perturbation is

$$U(t, t') = \sum_n [(-i)^n / n!] \int \dots \int_{t'}^t dt_1 dt_2 \dots dt_n T(H'(t_1) \dots H'(t_n)) = \exp(U_{oc}) U_L(t, t'),$$

where the unlinked terms are factored out⁷ to give a phase factor and only linked terms U_L will contribute to the cross section:

$$\sigma_{fi} = 2\pi |T_{fi}|^2 \rho_f,$$

where ρ_f is the final-state density divided by the incident flux, and

$$-2\pi i \delta(E_f - E_i - \omega) T_{fi} = \langle f | U_L(+\infty, -\infty) | i \rangle.$$

Each term in the expansion of T_{fi} can be represented by a diagram and can be evaluated using the orbital eigenstates generated by H_0 .

For the DEE process, the leading-order contributing terms have corresponding diagrams shown in Fig. 1. The important higher-order terms, similar to the ones in Fig. 1 but with exclusion-principle-violating⁵ hole-hole laddering between the two $2p$ -hole lines, are included in our calculation through the shifted-energy-denominator technique.⁵

Our calculated energy spectrum for the ejected electrons is shown in Fig. 2. Also shown is the

experimental curve of Carlson. The symmetric shape of the spectrum comes from counting both k and k' electrons. Since Carlson's data are not absolutely calibrated, we have normalized them to our curve. The general agreement between our result and experiment is excellent, but a detailed comparison is made difficult because of the uncertainties involved in the experimental data.⁸

Examination of the structure of the contributing terms leads one to expect the shape of the energy spectrum in Fig. 1 to be characteristic of general DEE processes. It also leads one to expect very small dependence on the incident x-ray energy for the total DEE cross section. Both conclusions are in agreement with experimental data.

Next we calculate the ratio of this DEE cross section to the total SEE cross section, $R = \text{Ne}^{++}(1s^2 2s^2 2p^4) / \text{Ne}^+(\text{total})$. We obtain a value $R = (11.1 \pm 0.4)\%$. In contrast, a previous theoretical estimate gives $R = 4.5\%$ from shakeoff theory.¹ The present calculation is again in excellent

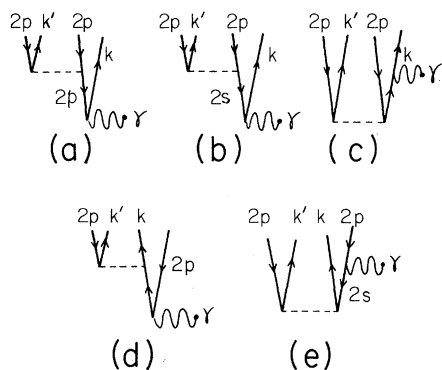


FIG. 1. The leading-order diagrams for the double electron ejection of neon.

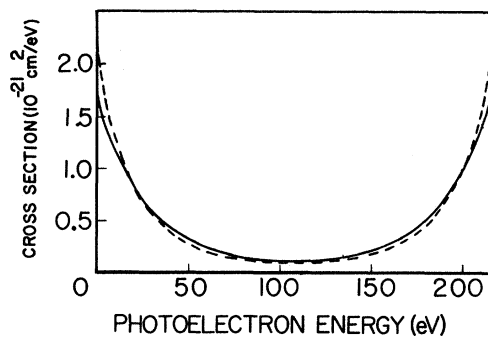


FIG. 2. Energy spectrum for the double electron ejection of neon. The solid curve is the present calculation and the dashed curve is from the experiment of Carlson.

agreement with the experimental result of Carlson¹ who obtained $R \simeq (11 \pm 1)\%$.⁹ Our result for the total $\text{Ne}^{++}(1s^2 2s^2 2p^4)$ excitation cross section is $(5.0 \pm 0.2) \times 10^{-20} \text{ cm}^2$.

Physical interpretations and discussions.—The interpretation of the physical processes associated with the diagrams are discussed below.

(1) Core rearrangement: The exclusion-principle-violating diagram in Fig. 1(a) represents the rearrangement effect of the remaining atomic electrons after the first $2p$ electron is photoejected into continuum k , resulting in the ejection of a second $2p$ electron into continuum k' . In our calculation, this effect alone gives $R = 5.2\%$. Thus it supports the validity of the sudden approximation employed in shakeoff theory which yields $R = 4.5\%$. The large discrepancy between the shakeoff theory and experiment comes from the following two additional processes.

(2) Virtual Auger transition: This process [diagram 1(b)] involves three orbital electrons. The photoionization of the $2s$ orbital to state k is followed by a virtual Auger transition,

$$\text{Ne}^+(1s^2 2s 2p^6) - \text{Ne}^{++}(1s^2 2s^2 2p^4) + e,$$

where two $2p$ electrons interact, with one going to the $2s$ orbital and the other being excited into continuum k' . This transition is "virtual" because it is energetically impossible to occur as a real process.

(3) Initial-state correlation: The diagram 1(c) represents the correlation effect between the two $2p$ electrons in the initial state. Although this amplitude is in itself smaller than the previous two processes, it contributes appreciably because of its strong constructive interference with diagram 1(a).

The diagram 1(d) represents the physical process of a direct collision between the outgoing photoelectron and another $2p$ orbital electron in the same atom. Diagram 1(e) represents initial-state correlations involving three electrons. Both are found to be negligible compared to 1(a), 1(b), and 1(c). As an indication of the contribution of the diagrams, the values of R are 5.2, 7.6, and 11.1% for 1(a), 1(a)+1(b), and 1(a)+1(b)+1(c), respectively.

Experiments on multiple photoionization have

long indicated that the process is intimately connected with electron-electron correlation effects. Progress toward a detailed study of this interesting phenomenon has been hampered by a lack of theoretical means for interpretation. The success of this calculation suggests that the MBPT approach can provide such a general framework for this class of problems. The MBPT approach is capable of even more detailed predictions, such as the angular distributions of the electrons. Experiments along this direction are most desirable and certainly within the present range of feasibility. A detailed study of the multiple photoionization process, in both theory and experiment, should prove to be most rewarding toward understanding the dynamic effects of electron-electron correlation in atoms.

*Work supported by the National Science Foundation and the National Aeronautics and Space Administration.
†Formerly R. T. Pu.

¹T. A. Carlson, Phys. Rev. **156**, 142 (1967).

²T. A. Carlson and M. O. Krause, Phys. Rev. **137**, A1655 (1965), and **140**, A1057 (1965), and **158**, 18 (1967); T. A. Carlson, M. O. Krause, and W. E. Modeman, J. Phys. (Paris), Colloq. **2**, 102 (1971).

³R. B. Cairns, H. Harrison, and R. I. Schoen, Phys. Rev. **183**, 52 (1969), and J. Chem. Phys. **53**, 96 (1970).

⁴T. W. Byron and C. J. Joachain, Phys. Rev. **164**, 1 (1967).

⁵H. P. Kelly, Phys. Rev. **131**, 684 (1963); R. T. Pu and E. S. Chang, Phys. Rev. **151**, 31 (1966); E. S. Chang, R. T. Pu, and T. P. Das, Phys. Rev. **174**, 1 (1968).

⁶T. N. Chang, T. Ishihara, and R. T. Poe, in *Sixth International Conference on the Physics of Electronic and Atomic Collisions. Abstracts of Papers, Boston, 1969* (Massachusetts Institute of Technology Press, Cambridge, Mass., 1969), p. 140; R. T. Poe, Bull. Amer. Phys. Soc. **16**, 487 (1971).

⁷P. Nozières, *Theory of Interacting Fermi Systems* (Benjamin, New York, 1964), p. 166.

⁸In Ref. 1 only the high-energy electrons due to the DEE process are observed. The experimental curve shown in Fig. 1 was obtained by subtracting out the contribution due to the DEE processes involving final ion states $1s^2 2s^2 2p^5$ and by assuming that the DEE energy distribution is the same for low- as for high-energy electrons.

⁹Carlson's experiment gives $\text{Ne}^{++}(\text{total})/\text{Ne}^+(\text{total}) = (14 \pm 1)\%$. The $\text{Ne}^{++}(\text{total})$ part contains about 10 to 20% of the $\text{Ne}^{++}(1s^2 2s^2 2p^6)$ configuration.